Proceedings of 3rd International Conference on Violent Flows (VF-2016)
9-11, March 2016, Osaka, Japan

Numerical Study on Liquid Sloshing in LNG Tanks Coupled with Ship Motion in Waves

Chonghong Yin, Yuan Zhuang, Decheng Wan*
State Key Laboratory of Ocean Engineering, School of Naval Architecture, Ocean and Civil Engineering, Shanghai Jiao Tong University, Collaborative Innovation Center for Advanced Ship and Deep-Sea Exploration, Shanghai, China
**e-mail dcwan@sjtu.edu.cn*

Abstract

In this paper, a LNG FPSO model is selected to study the liquid sloshing in two partially filled tanks coupled with ship motions in head waves. Numerical computations are performed by our in-house unsteady RANS solver, naoe-FOAM-SJTU, which is developed based on the open source tool libraries of OpenFOAM. The internal sloshing tanks and external waves are solved simultaneously. A VOF technique is used to capture free surface and deforming mesh is applied to treat the motion of LNG FPSO. The conditions in head wave with three different filling ratios in fore and aft tank: 0%~0%, 20%~20% and 30%~30% are performed first and compared with experiments. Then, LNG FPSO with conditions of tank filling ratios 57.5%~43.4 and 82.6%~23.5% in irregular wave is investigated. The results are compared with those without sloshing tanks. Numerical results are analyzed and compared with model experiments.

Keywords: LNG sloshing, naoe-FOAM-SJTU, RANS, VOF method, Nonlinear coupled motion

1 Introduction

With increasing energy demand and LNG FPSO production, liquid sloshing in LNG tanks excited by the ship motion in waves is a crucial issue faced in engineering applications and has become one of the most important research interests in the fields of ocean engineering and ship hydrodynamics. The sloshing of partially filled LNG tanks has large effects on the motion of ship. In return, the ship motions also influence the excited sloshing. The coupling effect of sloshing tanks and ship motions is still an important research problem.

Recent years, with the rapid development of computer technology, Computational fluid dynamics (CFD) has become a powerful numerical tool to simulate the coupling effects of ship motion and tank sloshing. In CFD computations, the viscosity effects of fluid can be fully taken into consideration and non-linear factors can be handled precisely, especially in the conditions of high Reynolds number. Therefore, it’s possible to simulate ship motions in sea waves coupled with LNG tank sloshing by CFD methods.

Many studies have been carried out on tank sloshing coupled with ship motions based on both numerical and experimental methods. B. Nam, *et al*. [1] performed both experimental and numerical studies of a LNG FPSO coupled with sloshing tanks in head and beam waves. The numerical study is done by impulse-response-function (IRF) for ship motion and by finite-difference method for internal liquid sloshing. Also, the numerical study extends to the observation of pressure field inside the tanks. Y. Kim, et al. [2] applied the same methods to investigate the roll motion of a modified S175 hull equipped with rectangular anti-rolling tank, considering the coupling effects of ship motion and sloshing. Z. Shen, *et al.* [3] made numerical simulations of the KVLCC2 tanker fully coupled with LNG sloshing in waves, computations are performed by the unsteady RANS solver, naoe-FOAM-SJTU. The modified KVLCC2 is investigated in both head and beam waves with two filling ratios of tank, results are compared with those without sloshing tanks and comparison denotes quite different characteristics of motions in those two conditions. C. Yang, *et al.* [4] used a further developed Volume of Fluid (VOF) technique coupled with an incompressible Euler/Navier Stokes solver to simulate the interactions of extreme waves and a LNG carrier with full or partially filled tanks with adaptive, unstructured grids. An arbitrary Lagrangian-Eulerian (ALE) was used to treat the motions of ship. However, the turbulent effects were neglected in the work. X. Li, *et al.* [5] also preformed simulations to calculate the coupling effects of ship motion and tank sloshing. The radiation force is integrated by using IRF approach. The liquid motion in the tank is simulated by CFD method. Response amplitude operators (RAOs) of the ship coupled with tank at different filling levels is obtained both in time domain and frequency domain.

The object of this paper is to numerically investigate ship motions coupled with inside tank sloshing by CFD methods. The internal sloshing tank and external sea waves are treated as an entire computational region. A Reynolds-Averaged Navier-Stokes (RANS) solved in both two regions simultaneously, applying SST turbulence model [6]. Volume of fluid (VOF) method is used to capture both sloshing liquid and outside wave surface. The forces and moments from both tank sloshing and external wave are integrated together to predict ship motions.

All computations are performed by our in-house unsteady RANS solver naoe-FOAM-SJTU, which is based and developed on the open source tool packages, OpenFOAM [7]. Previous works have made many progresses in developing and validating this solver applied in this paper. Shen *et al.* [8] simulated the viscous flow acting on KVLCC2, KCS, and DTMB5415 and compared with the measurement results by naoe-FOAM-SJTU. Ye *et al.* [9] computed the added resistance in regular head waves with ship trim and sinkage, and validated the ability of naoe-FOAM-SJTU to solve the strongly nonlinear problems. Liu *et al.* [10] used naoe-FOAM-SJTU to simulate motion responses of an offshore observation platform in regular waves. Shen *et al.* [11] also implemented the dynamic overset grid technique into the code, which made the solver more appropriate for various kinds of complex hydrodynamic issues of naval architecture and ocean engineering.

The paper is organized as follows. The description of computational methods is presented first, and is followed by the geometry and conditions. The results are then presented and discussed. Finally, a summary and conclusions are provided.

2 Numerical Methods

2.1 Governing Equations

In this paper, Reynolds-Average Navier-Stokes (RANS) equations coupled with VOF method are adopted for incompressible viscous fluid flows in sloshing tanks. The governing equations are:

$$\nabla \cdot \mathbf{U} = 0 \tag{1}$$

$$\frac{\partial \rho \mathbf{U}}{\partial t} + \nabla \cdot \left(\rho\left(\mathbf{U} - \mathbf{U}_g\right)\mathbf{U}\right) = -\nabla p_d - \mathbf{g} \cdot \mathbf{x} \nabla \rho + \nabla \cdot \left(\mu_{\mathrm{eff}} \nabla \mathbf{U}\right) + \left(\nabla \mathbf{U}\right) \cdot \nabla \mu_{\mathrm{eff}} + f_\sigma + f_s \tag{2}$$

where $\mathbf{U}$ is velocity field; $\mathbf{U}_g$ is velocity of grid nodes; $p_d = p - \rho \mathbf{g} \cdot \mathbf{x}$ is dynamic pressure, subtracting hydrostatic component from total pressure; ρ is the mixture density with two phases; $\mathbf{g}$ is the gravity acceleration vector; $\mu_{\mathrm{eff}} = \rho(\nu + \nu_t)$ is effective dynamic viscosity, in which ν and ν_t are kinematic viscosity and eddy viscosity respectively; ν_t is obtained by $k-\omega$ SST turbulence model; f_σ is the surface tension term in two phases model.

The solution of momentum and continuity equations is achieved by using the pressure-implicit split-operator (PISO) algorithm. This method uses a predictor-corrector method to solve the Navier-Stokes equations by applying the continuity equation, utilizing a collocated grid method.

2.2 VOF Method

A VOF method with bounded compression techniques is applied in this paper. The advantage of this formulation is that it can control numerical diffusion and capture the interface with higher resolution. The VOF transport equation is expressed as:

$$\frac{\partial \alpha}{\partial t} + \nabla \cdot \left[\left(\mathbf{U} - \mathbf{U}_g\right)\alpha\right] + \nabla \cdot \left[\mathbf{U}_r\left(1-\alpha\right)\alpha\right] = 0 \tag{3}$$

where α is volume of fraction, indicating the relative proportion of fluid in each cell and its value is always between zero and one:

$$\begin{cases} \alpha = 0 & \text{air} \\ \alpha = 1 & \text{water} \\ 0 < \alpha < 1 & \text{interface} \end{cases} \tag{4}$$

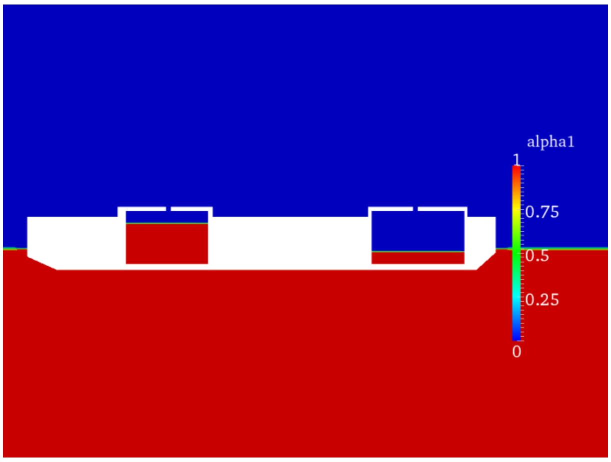

Fig. 1 Set fields of water for LNG FPSO tank filling rate 82.6%~23.5% by VOF method

2.3 Wave Generation

The wave generation method applied is to impose the boundary conditions α in VOF equation (3) and $\mathbf{U}(u,v,w)$ in RANS equations (2). The expressions of boundary conditions can be given by the linear deep-water wave theory:

$$\begin{aligned} \zeta(x,t) &= a\cos(kx - \omega_e t) \\ u(x,y,z,t) &= U_0 + a\omega e^{kz}\cos\beta\cos\theta \\ v(x,y,z,t) &= a\omega e^{kz}\sin\beta\cos\theta \\ w(x,y,z,t) &= a\omega e^{kz}\sin\theta \end{aligned} \tag{5}$$

in which, $\theta = k\cos\beta \cdot x + k\sin\beta \cdot y - \omega_e t$; ζ is transient wave elevation; a is wave amplitude; k is wave number; U_0 is velocity of ship; ω is natural frequency of wave; ω_e is encounter frequency, given by $\omega_e = \omega + kU_0 \cos\beta$; β is wave direction, $\beta = 0$ represents head wave.

2.4 6DoF Motions

A 6DoF motion module is developed to predict the motions of ship. In this method, two coordinate systems are used to solve 6DoF equation. One system is earth-fixed system and the other is body-fixed system. Forces and moments are calculated first in the earth-fixed system and transformed into body-fixed system. Next, the rigid body equations are solved to obtain the acceleration, converted to earth-fixed system and integrated to velocity and displacement. Finally, solve the Laplace equation with variable diffusivity to obtain global mesh movement.

3 Ship Geometry and Conditions

3.1 Ship Model

The ship model chosen in this paper is a LNG FPSO, the model experiment was carried out at the towing tank in Seoul National University by B. Nam, *et al.* [1]. The experiment geometry and principle dimensions are illustrated in Fig. 2 and Table 1.

The length, breadth and draft of FPSO are 285.0m, 63.0m and 13.0m, respectively. The displacement volume of LNG FPSO is 220,017.6 m^3. The length, breadth and height of the fore tank and the aft tank are 49.68m, 46.92m, 32.23m and 56.62m, 46.92m, 32.23m respectively. The distance from the bottom of tank to the keel line is 3.3m. The experimental and computational ship model is 1/100 scale of the full scale LNG FPSO.

Table 1 Principle Dimensions of LNG FPSO

			
Main particulars		Full Scale	Model
Scale factor	—	1	1/100
Length between perpendiculars	L_{PP} (m)	285	2.85
Maximum beam of waterline	B_{WL} (m)	63	0.63
Draft	T (m)	13	0.13
Displacement	Δ (m^3)	220017.6	220.0176
Natural period of roll	T_ϕ (s)	13	1.3
Vertical Center of Gravity (from keel)	KG (m)	16.5	0.165
Radius of gyration	K_{xx}	19.45	0.1945
	K_{yy}	71.25	0.7125

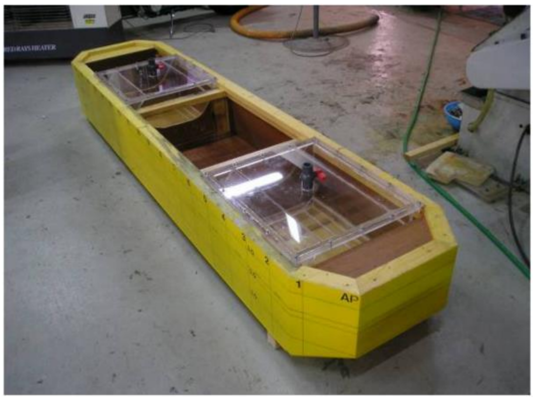

(a) Model ship

(b) Model tank

Fig. 2 Geometry of LNG FPSO[1]

Fig. 3 shows the different liquid depth of fore (FP) and aft (AP) tank. The computations were carried out at five different filling conditions: 0%~0% (FP-AP, which means no sloshing), 20%~20%, 30%~30%, 57.5%~43.3% and 82.6%~23.5%. Drafts at FP and AP were kept constant at each filling condition, also kept the longitudinal moment inertia same.

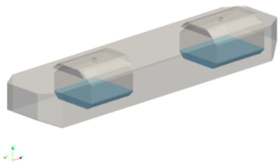

(a) 20%~20%

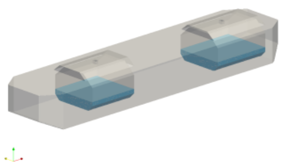

(b) 30%~30%

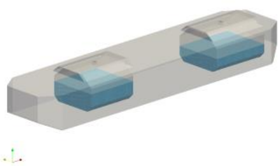

(c) 57.5%~43.3%

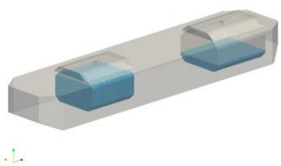

(d) 82.6%~23.5%

Fig. 3 Geometry of LNG FPSO equipped with LNG tanks

3.2 Mesh and computation domain

For numerical computations in this paper, a same computing domain is used. The space coordinate range is determined as:

$$-2.0L_{pp}<x<4.0L_{pp},$$

$$-1.5L_{pp}<y<1.5L_{pp},$$

$$-1.0L_{pp}<z<1.0L_{pp};$$

The mesh is generated by *SnappyHexMesh*, an automatic mesh generation tool provided by OpenFOAM. This tool generates mesh based on Cartesian grids by splitting hexahedral cells, resulting in unstructured octree hexahedral grids. Fig. 4 shows the details of generated hull mesh.

The numbers of cells are 1.7M for head wave computations. The LNG tanks require additional 0.5M cells. Besides, two small tunnels are used to connect the LNG tanks with external region. The aim of this treatment is to avoid setting reference pressure inside the tanks and simplify the computations with minimum influence on computational results.

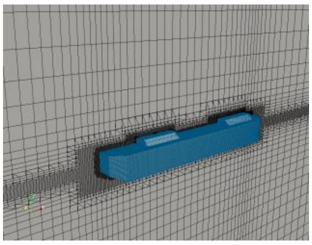
(a) bow

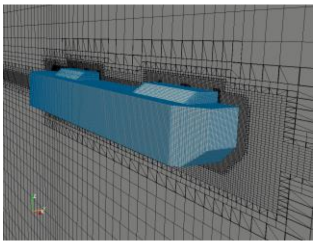
(b) stern

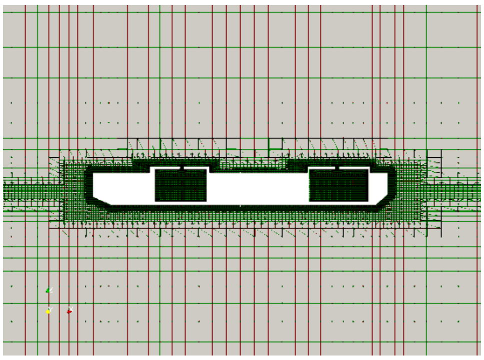
(c) ship hull with tanks

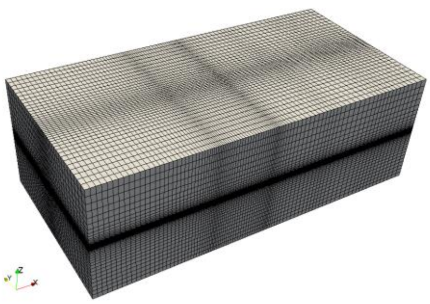
(d) background mesh

Fig. 4 Mesh generation

4 Results and Analysis

4.1 Regular wave conditions

Simulations at regular wave conditions are carried out firstly and numerical results are compared with model test. Parameters of regular wave in test conditions are shown in Table 2. Same to the experiment, wave height was fixed to 0.025m. λ/L_{pp} =1.005, which represents the wave length normalized by ship length.

Table 2 Parameters of regular wave

No	filling ratios	Wave height	wave length	encounter frequency
		H (m)	λ	f_e (Hz)
1	0%~0%	0.025	2.8651	4.6382
2	20%~20%	0.025	2.8651	4.6382
3	30%~30%	0.025	2.8651	4.6382
4	57.5%~43.3%	0.025	2.8651	4.6382
5	82.6%~23.5%	0.025	2.8651	4.6382

In order to investigate the motions response quantitatively, the computational results are analyzed by transfer function. The definition of transfer functions of heave and pitch motions can be given as:

$$TF_3 = \frac{x_{31}}{a} \qquad TF_5 = \frac{x_{51}}{ak}$$

where, TF_3 and TF_5 are the transfer functions of heave and pitch motions, respectively; x_{31} and x_{51} are the 1st harmonic amplitude of heave and pitch motions, obtained by Fourier Series (FS); a is wave amplitude and ak is wave steepness.

The results comparisons are shown in Table 3. The experimental data come from [1]. It shows that the predicted transfer functions fairly agree with the measurements for pitch motions at different filling ratios, but the predicted transfer functions for heave motions are 25% larger than EFD data. Time histories of heave and pitch motions of different filling ratios are shown in Fig. 5. Comparisons show little difference among five filling ratios for heave motion, but larger difference for pitch motion. Filling ratios 57.5%~43.3% and 82.6%~23.5% have more significant coupling effects of tank sloshing and ship pitch motion, the largest pitch motion amplitudes are 21% and 18% larger than condition without sloshing, respectively.

Table 3 Results comparisons

No	filling ratios	TF_3		TF_5	
		EFD	CFD	EFD	CFD
1	0%~0%	0.140	0.178	0.737	0.723
2	20%~20%	0.140	0.180	0.724	0.729
3	30%~30%	0.140	0.178	0.810	0.758
4	57.5%~43.3%	—	0.159	—	0.781
5	82.6%~23.5%	—	0.182	—	0.806

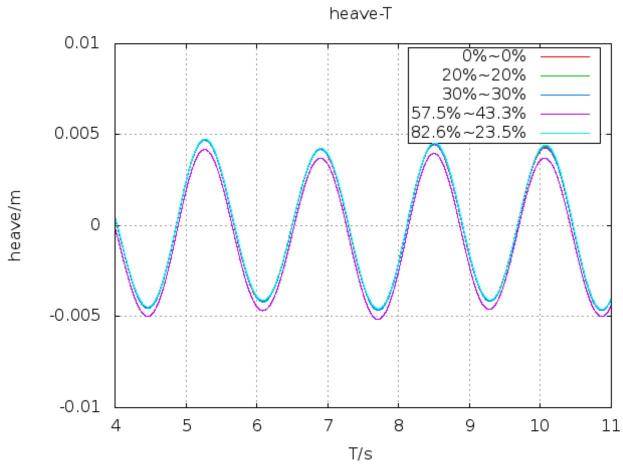

(a) Heave motion

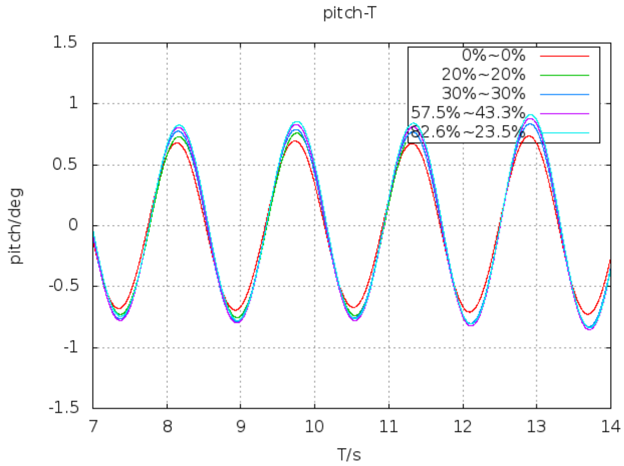

(b) Pitch motion

Fig. 5 Time history of heave and pitch motions with different filling ratios

4.2 Irregular wave conditions

Filling ratios 57.5%~43.3% and 82.6%~23.5% conditions are studied further in this part, and compared with the 0%~0% filling condition. All the irregular waves in this study are generated through the two parameters ITTC spectrum. The range of working frequency $f_{e,max}$ and $f_{e,min}$ are 3.1831, 0.3183 respectively. The 1/3 significant wave height is set to 0.14m and characteristic period is 3s. In this part, the ship has a forward speed of Fr = 0.076 while it has zero speed for regular wave conditions.

Time histories of heave and pitch motions of different filling ratios in irregular wave conditions are shown in Fig. 6. Same with regular wave conditions, comparisons with no sloshing condition show little difference for heave motion, but larger difference for pitch motion, especially at the peak and trough of the wave. The coupling effect made larger amplitude for pitch motion.

Fig. 7 shows four snapshots of LNG FPSO motion in irregular wave with filling ratio 82.6%~23.5% in one period (3s). Because of the different filling rate for AP and FP tank, the liquid sloshing in two LNG tanks also exist phase difference. The AP tank was taken as an example for analysis here. At t/T=0, the LNG stays at the balanced position. At t/T=0.25, the trough of wave reaches and the bow nearly buries into wave, the sloshing liquid in LNG tank (AP) moves from bow to stern. At t/T=0.50, the wave peak reaches ship bow and the bow goes up, the bow reaches the highest position and nearly goes out of water. At the same time, liquid in LNG tank (AP) begin to move from stern to bow fast. At t/T=0.75, the wave peak passes by and the ship returns to balanced position, while the sloshing liquid just arrived at the far front of the LNG tank (AP) bulkhead, the liquid with forward direction movement changed to vertical instantaneously by the obstacle of the bulkhead, and form a jet. In this process, the liquid move upward along the bulkhead, also produce a slamming.

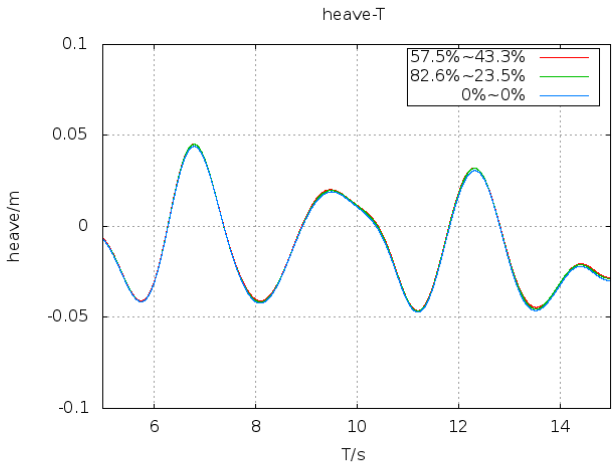

(a) Heave motion

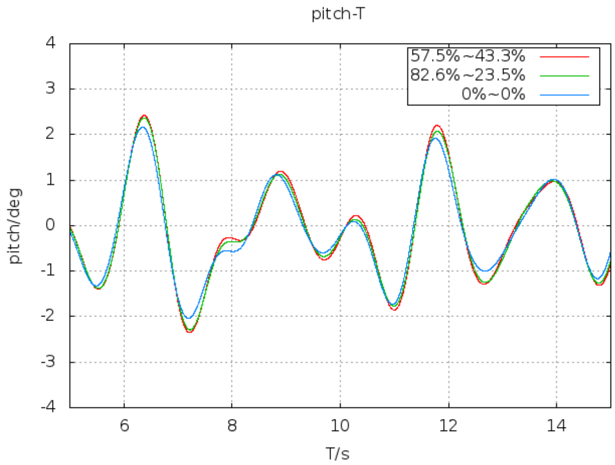

(b) Pitch motion

Fig. 6 Time history of heave and pitch motions with different filling ratios

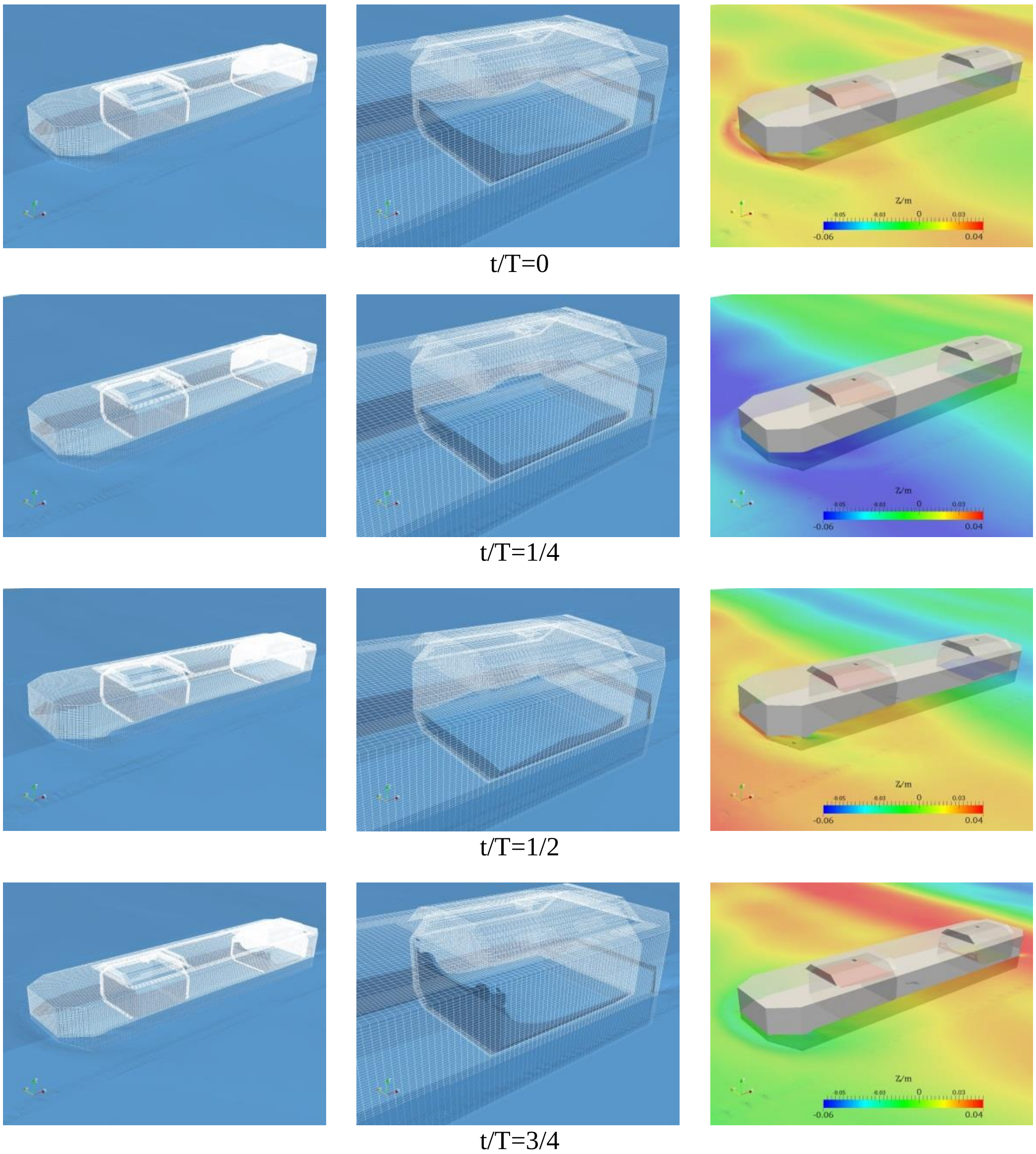

Fig.7 Four snapshots of LNG FPSO motion in irregular wave with filling ratio 82.6%~23.5% (From left to right is global view of LNG FPSO, detail view of the aft tank sloshing and view of free surface in turn)

5 Conclusion

In this paper, numerical simulations of the LNG FPSO fully coupled with liquid sloshing in waves are presented. The computations are performed by the solver naoe-FOAM-SJTU, which is developed based on open source CFD package, OpenFOAM. The internal tank sloshing and external wave flow are computed simultaneously by solving RANS equations. VOF is used to capture the two phases interface. Two wave conditions are considered in this paper, regular wave and irregular wave.

First of all, simulations of LNG FPSO model with different filling ratios at regular wave condition are performed and compared with existing measurements data. Results indicate faire agreement with measurements. Secondly, the coupling effects at irregular wave condition are studied further. The computational results show that in the condition of wave length equal to ship length, the sloshing has little effect on the heave motion in head wave, but larger influence on pitch motion. The period of pitch and heave motion has an obvious different with the tank natural period, so the hull motion didn't cause tank liquid resonance under the head sea conditions.

However, in current stage, only the head wave condition is considered, the sloshing will have more notable effects on roll motion in beam wave, which will be studied further. Also, only one wave length is considered in this paper, therefore, more wave lengths need to be computed in the future work to fully investigate the problem of ship motion coupled with LNG sloshing.

Acknowledgements

This work is supported by National Natural Science Foundation of China (Grant Nos. 51379125, 51490675, 11432009, 51411130131), The National Key Basic

Research Development Plan (973 Plan) Project of China (Grant No. 2013CB036103), High Technology of Marine Research Project of The Ministry of Industry and Information Technology of China and the Program for Professor of Special Appointment (Eastern Scholar) at Shanghai Institutions of Higher Learning(Grant No. 2013022), to which the authors are most grateful.

References

[1] Nam. B. *et al.* (2009) "Experimental and numerical studies on ship motion responses coupled with sloshing in waves," Journal of Ship Research, vol. 53, pp. 68-82

[2] Y. Kim. *et al*. (2007) "Study on coupling effects of ship motion and sloshing," Ocean Engineering, vol. 34, pp. 2176-2187

[3] Shen. Z. *et al.* (2012) "Numerical Simulations of Large-Amplitude Motions of KVLCC2 Coupled with Sloshing in Waves," *Proc. of International Conference on Violent Flows*, Nantes, France, pp 25-27

[4] C. Yang. *et al.* (2006) "An unstructured-grid based volume-of-fluid method for extreme wave and freely-floating structure interactions," Journal of Hydrodynamics, vol. 18, pp. 415-422

[5] Xu L. *et al.* (2014) "Numerical analysis of ship motion coupled with tank sloshing," *Proc. of International Conference Oceans,* Taipei, China, pp 1-10

[6] F. Menter. (1994) "Two-equation eddy-viscosity turbulence models for engineering applications," AIAA Journal, vol. 32, pp. 1598-1605

[7] Jasak H. (2009) "OpenFOAM: Open source CFD in research and industry". International Journal of Naval Architecture and Ocean Engineering, 1(2): 89-94

[8] Shen Z. *et al.* (2012) "Motion response and added resistance of ship in head waves based on RANS simulations". Chinese Journal of Hydrodynamics, 27(6): 621-633

[9] Ye H. *et al.* (2012) "Numerical prediction of added resistance and vertical ship motions in regular head waves". Journal of Marine Science and Application, 11(4): 410-416

[10] Liu Y. *et al.* (2013) "Numerical simulation of motion response of an offshore observation platform in waves". Journal of Marine Science and Application, 1(12): 89-97

[11] Shen Z. *et al.* (2015) "Dynamic overset grids in OpenFOAM with application to KCS self-propulsion and maneuvering". Ocean Engineering, 108: 287-306.